Current Natural Sciences & Engineering
Volume 3, Issue 1, 2026, 946-953

Analysis of Effects of Different Loads on Diversity Parameters of a 4-port Multiband MIMO Antenna

Shailesh[1], Abhishek Kumar[1], Jyotsna Gaur[1], Amit Birwal[1], and Kamlesh Patel*[1]

Department of Electronic Science, University of Delhi South Campus, New Delhi-110021, India

Received date:30/04/2026, Acceptance date: 17/06/2026

DOI: **http://doi.org/10.63015/8ms-2504.3.1**

**Corresponding author: :* kpatel@south.du.ac.in

Abstract

This work investigates the effects of different loads on the diversity parameters of a multiband multiple-input multiple-output (MIMO) antenna. The unused ports of a 4-port multiband MIMO antenna are terminated with a matched load, an open load, or a short load when exciting one or two ports. The diversity parameters of MIMO antenna, such as Envelope Correlation Coefficient (ECC), Diversity Gain (DG), Total Active Reflection Coefficient (TARC), and Mean Effective Gain (MEG), are calculated using S-parameters. The maximum ECC values are 0.311, 0.314, and 0.302, and the minimum TARC values are -8.272 dB, -8.223 dB, and -8.035 dB, respectively, in the operating bands for these three loads. The DG is approximately 10 dB, and the MEG ratios are within ±3 dB across 4-6 GHz for the three different loads. Generally, the open load shows weak participation, while the short load offers strong coupling and severe diversity degradation. In the present study, the effects of these different loads are found to be negligible on the diversity parameters of the multiband MIMO antenna.

Keywords: S-parameters, MIMO Antenna, Diversity parameters, Multiband, System performance.

1. Introduction

In practice, each port of a Multiple-Input Multiple-Output (MIMO) antenna system is not isolated. It is connected to RF front-end circuits, matching networks, active components (LNAs, PAs, switches), etc. These introduce different load impedances, which are not always perfect 50 Ω. In real scenarios, instead of assuming all ports are perfectly matched, one should study the MIMO antenna performances with matched loads (50 Ω), mismatched loads, and open/short conditions to assess the reliability of the MIMO system. Most reported MIMO antennas assume that all inactive ports are terminated with a standard matched load and evaluate performance under ideal excitation conditions [1] [2] [3] [4] [5] [6]. However, in practical scenarios such as switching networks, reconfigurable systems, or fault conditions, antennas may experience open-circuit, short-circuit, or mismatched load states. The influence of these non-ideal terminations on key MIMO performance parameters, such as envelope correlation coefficient (ECC), diversity gain (DG), mean effective gain (MEG), and total active reflection coefficient (TARC), has not been systematically investigated in existing literature. Therefore, a clear research gap exists in analyzing and comparing MIMO antenna performance under matched load, open-circuit, and short-circuit conditions. So, the experimental validity of MIMO diversity performance is important to better understand robustness and real-world operational behaviour under the mismatch conditions at the ports of MIMO antenna or system.

In such a MIMO antenna system, diversity characteristics—such as the ECC, DG, TARC, and MEG—depend heavily on how independently the antenna elements operate. Introducing short and open loads (intentional or due to faults/mismatches) significantly alters these characteristics. The degree of correlation between the communication channels of the MIMO antenna is known as the envelope correlation coefficient (ECC) [7]. The ECC is expressed in terms of the radiation field patterns of the two-port diversity system as given in equation (1) [8]. Here, E^* is a complex conjugate of the electric field (E) pattern of the MIMO antenna for the θ and ϕ directions, and XPR is the cross-polarization ratio, which is the ratio of power in the co-polarized field to the cross-polarized field. The P_θ and P_ϕ are the angular power density in θ and ϕ directions, respectively. Although the ideal ECC value for a fully uncorrelated MIMO antenna is zero, an acceptable diversity performance requires a value between 0 and 0.5.

$$ECC_{ij} = \frac{\left|\oiint\left[XPR.E_{\theta_i}E^*_{\theta_j}P_\theta+E_{\phi_i}E^*_{\phi_j}P_\phi\right]d\Omega\right|^2}{\{\oiint\left[XPR.E_{\theta_i}E^*_{\theta_i}P_\theta+E_{\phi_i}E^*_{\phi_i}P_\phi\right]d\Omega\times \oiint\left[XPR.E_{\theta_j}E^*_{\theta_j}P_\theta+E_{\phi_j}E^*_{\phi_j}P_\phi\right]d\Omega\}} \quad (1)$$

In terms of S-parameters, ECC can be obtained using equation (2) for the 2-port MIMO antenna:

$$\rho_e = \frac{|S^*_{11}S_{12}+S^*_{21}S_{22}|^2}{(1-|S_{11}|^2-|S_{21}|^2)(1-|S_{22}|^2-|S_{12}|^2)} \quad ((2)$$

When any port is either open ($S_{ii} \rightarrow 1$) (high reflection) or short ($S_{ii} \rightarrow -1$), numerator correlation terms increase and reduce denominator efficiency, which leads to higher ECC.

The Diversity Gain (DG) of the MIMO system is the next essential parameter to evaluate its diversity performance. Equation (3) provides an expression to find DG using ECC [8].

$$DG_{ij} = 10\sqrt{1 - \left(ECC_{ij}\right)^2} \quad (3)$$

With open or short loads at any port, DG drops as ECC increases. So the significant degradation in the MIMO performance is due to high correlation and reduced independent signal paths.

When operating multiple AEs simultaneously, the closely spaced AEs affect the system's performance, including gain, bandwidth, and efficiency. For this reason, the Total Active Reflection Coefficient (TARC) is a crucial metric for assessing the diversity performance of a MIMO antenna. To calculate TARC, the square root of the ratio of total reflected power to total incident power is taken as shown in equation (4). For an N×N MIMO antenna, TARC is defined as:

$$\text{TARC} = \sqrt{\frac{\sum_{i=1}^{N} \left| \sum_{k=1}^{N} S_{ik} e^{j\theta_k} \right|^2}{N}} \quad (4)$$

Where, N is the antenna ports, S_{ik}= S-parameters having i and k as the receiving port and transmitting port, respectively, and θ_k= phase of the excitation signal at port k.

The four-port MIMO/Diversity system's S-parameters can be used to produce TARC using equation (5), where θ_i presents the phase of the associated transmission (S_{mn}) parameter, i=1, 2, 3 [9] and ranges from 0 to 2π, m, n= 1, 2, 3, 4 for the four-port antenna. The TARC is preferred to be less than -10 dB for the perfect MIMO system. The open load at any port leads to a moderate increase in TARC due to full reflection but weaker coupling, while the short load leads to a severe increase in TARC due to strong coupling and phase inversion. As a result, both kinds of load degrade MIMO performance.

$$TARC = \sqrt{\frac{\sum_{i=1}^{4} \left| \sum_{k=1}^{4} S_{ik} e^{j\theta_k} \right|^2}{4}} \quad (5)$$

By utilizing the following equation (6) [8], the Mean Effective Gain (MEG) of the designed spatial diversity MIMO antenna for each port (Port 1, Port 2, Port 3, and Port 4) can be calculated. The MEG ratio (MEG_i/MEG_j) should be within ±3 dB for optimal diversity [10], i, j, k = 1, 2, 3, 4.

$$MEG_k = 0.5[1 - |S_{k1}|^2 - |S_{k2}|^2 - |S_{k3}|^2 - |S_{k4}|^2] \quad (6)$$

MEG becomes imbalanced when the MIMO antenna is terminated open or short at any port, resulting in the active element dominating and the open element contributing negligibly.

Thus, the efficiency of the MIMO system is reduced by power loss due to dissipation in short circuits and re-radiation with phase distortion. Another effect is the resonance shift as the shorted antenna element acts as a reactive load, which detunes the system. In this paper, an experimental study is conducted on diversity parameters, which are calculated from measured S-parameters. These S-parameters are obtained for a 4-port multiband MIMO antenna with matched, open, and short loads. Analysis of changes in diversity parameters is presented for the reliability of such an MIMO system.

2. Detail of the multiband MIMO antenna:

Fig. 1(a) depicts the proposed antenna's design, consisting of four antenna elements (AEs) operating at the four different 5G bands for the lower and mid-frequency ranges. The blue color shows the Cu layer, while the green color represents the etched area of the antenna schematic. A single-sided FR-4 substrate (ε_r = 4.3, tanδ = 0.02) measuring 150 × 120 × 1.5 mm^3 is used to design the proposed antenna. The other dimensions (in mm) of this antenna are R=54, R2=44, F1=4, F2=3.8, F3=1.5, F4=1.2, G1=1, G2=1, G3=0.3, G4=0.5, G5=0.4, G6=0.6, W1=3.9, L1=3.9, W2=4.5, L2=18.2, W3=6.06, L3=10, W4=4.5, L4=10, W5=2, L5=5, and W6=9.7. It was fabricated and coated with a protective green layer, as shown in Fig. 1(b). The four antenna elements (AEs) are positioned at their four edges on the substrate's front side. AE1 is designed to cover the lower 5G band (<1 GHz), and the other three AEs, AE2, AE3, and AE4, cover different mid-frequency bands up to 6 GHz. To achieve high isolation between AE1 and AE2, a meander-line decoupling structure (DS) is integrated into the ground on the right side of AE1.

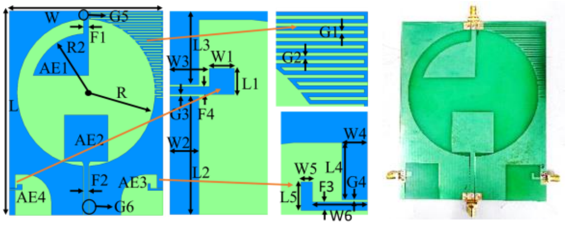

Figure 1: Multi-band antenna (a) Schematic, (b) Actual photograph

In Fig. 1(a), AE1 offers a bandwidth of 0.55-0.89 GHz, AE2 offers a bandwidth of 1.27-2.82 GHz, AE3 provides an additional band of 3.05-4.34 GHz, and AE4 provides a final band of 4.47-6 GHz. Isolation between the AEs is shown in Fig. 1(b) when AE1 is excited. The isolation between AE1 and AE2 was>10 dB and >20 dB from AE3 and AE4, respectively, across the entire band up to 6 GHz.

The simulated responses of four AEs are shown in Fig. 2(a)-(d), which were obtained using the CST Microwave Studio software. The return loss levels well below -10 dB at the four intended bands (0.72-0.98 GHz, 1.62-2.66 GHz, 3.04-4.42 GHz, and 4.47-6 GHz). The inter-element isolation parameters show that the AEs exhibit high isolation performance, exceeding 15.01 dB throughout the four bands. Gains of 1.44 to 3.8 dB, 1.728 to 5.065 dB, 1 to 3.066 dB, and 2.75 to 4.61 dB are offered by the AE1, AE2, AE3, and AE4, respectively. The efficiency of AE1, AE2, AE3, and AE4 is 61.67-72.99%, 72.37-85.64%, 55.89-64.98%, and 67.93-80.07%, respectively.

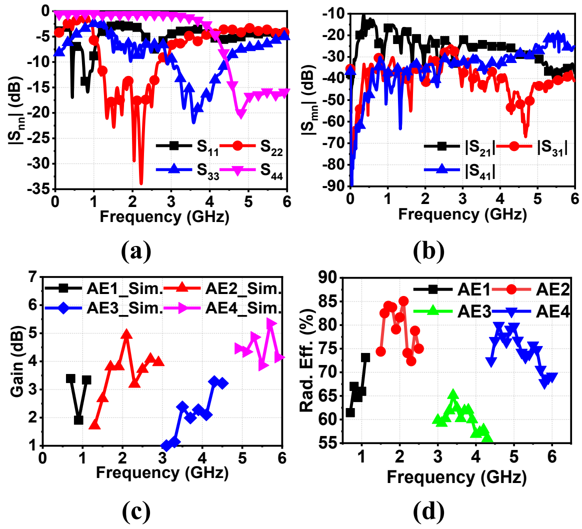

Figure 2: Simulation response of multi-band antenna (a) Reflection coefficient (S_{nn}), (b) Isolation (S_{mn}), (c) Gain, and (d) Efficiency.

Fig. 2 (c) displays the simulated gains of 1.44 to 3.8 dB, 1.728 to 5.065 dB, 1 to 3.066 dB, and 2.75 to 4.61 dB offered by the AE1, AE2, AE3, and AE4, respectively, at the four frequency bands over their corresponding operating ranges. Fig. 2(d) displays the simulated efficiencies of the AE1, AE2, AE3, and AE4, which are 61.67-72.99%, 72.37-85.64%, 55.89-64.98%, and 67.93-80.07%, respectively at the four respective operating bands.

2. Antenna Measurements with Different Loads:

The characteristics of the multiband antenna are measured with different loads upto 6 GHz using the Transcom T6 Vector network analyser (VNA). The setup is shown in Fig. 3, and S-parameters are measured by placing different types of loads on the multiband antenna's open ports after calibration. For measuring the S_{11} reflection parameter, the VNA's port 1 is connected to port 1 of the multiband antenna, while ports 2-4 of the multiband antenna are connected to matched loads. Then, S_{11} is measured by replacing matched loads with short terminations, and the final S_{11} readings are obtained with open terminations on ports 2 to 4 of the multiband antenna. These measured S_{11} parameters are compared with the simulated S_{11} in Fig. 4(a). Similarly, other transmission S-parameters (S_{21}, S_{31}, and S_{41}) are measured with different loads and presented in Fig. 4(b-d).

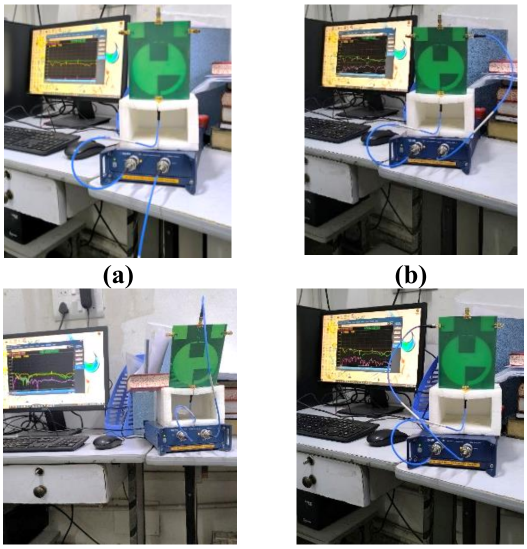

Figure 3: VNA setup of multi-band antenna (a) S_{11} measurement, (b) S_{21} measurement, (c) S_{31} measurement, and (d) S_{41} measurement.

3.1 Effect of different loads on S-parameters of multiband antenna:

The S-parameter responses, such as S_{11}, S_{21}, S_{31}, and S_{41}, of the multiband antenna with different loads are plotted in Figure 4. No significant differences in the S-parameters with different loads are observed compared to the simulated responses. This confirms that the effects on S-parameters are negligible due to different loads, since all ports operate over different frequency ranges. Also, the proposed antenna provides stable impedance matching, high isolation irrespective of whether the inactive ports are terminated with matched loads, open circuits or short circuits. This shows the robustness of the proposed antenna design for practical MIMO wireless communication applications. The small discrepancies between simulated and measured results are mainly due to fabrication tolerances, SMA connector soldering imperfections, and measurement uncertainties during VNA characterization. Additionally, the slight differences are caused due to differences in the dielectric constant, surface roughness and thickness of the FR-4 board. Regardless, the measured results have a good correspondence with the simulated data; hence, the effectiveness of the designed multiband MIMO antenna is proven.

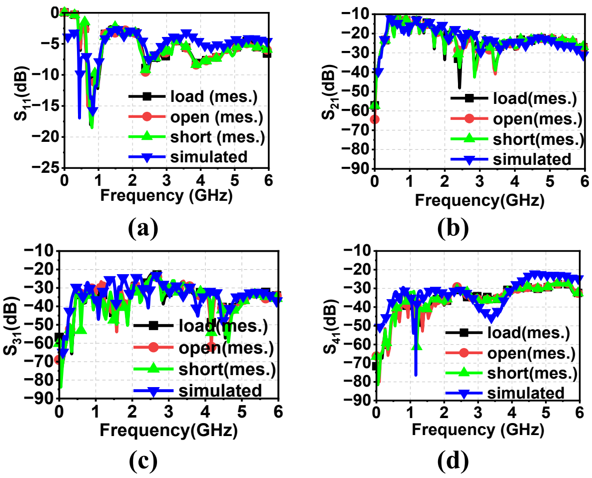

Figure 4: S-parameter responses of multiband antenna with different loads (a) S_{11} response, (b) S_{21} response, (c) S_{31} response, and (d) S_{41} response.

3.2 Effect of Different on Diversity Parameters of Multiband Antennas:

This section examines the various diversity parameters of the utilized multiband MIMO antenna, which are obtained from the measured S-parameters. Fig. 5(a) displays that the ECC values between ports 1-2, 1-3, and 1-4 are below 0.311, 0.314, and 0.302 in the operating bands for matched, open, and short load, respectively. The ECC values of ~0.3 (in <50 MHz bandwidth) indicate moderate correlation between AE1 and AE2 due to nearby operating bands. For other two AEs, ECC values are well below 0.02. So, the proposed antenna can still support diversity operation, even if the correlation level may slightly reduce channel capacity and DG compared to highly decoupled MIMO systems. The DG is approximately 10 dB, as shown in Fig. 5(b). Additionally, the plots show that the presented MIMO antenna provides good spatial diversity across the operating bandwidth, with similar high DG and low ECC for all three loads.

Fig. 5(c) plots the TARC results as a function of frequency for the three cases (Case 1=$\theta_1 = 0^{\circ}, \theta_2 = 90^{\circ}, \theta_3 = 180^{\circ}$; Case2=$\theta_1 = 0^{\circ}, \theta_2 = 90^{\circ}, \theta_3 = 270^{\circ}$; Case3=$\theta_1 = 0^{\circ}, \theta_2 = 180^{\circ}, \theta_3 = 90^{\circ}$) using equation (5). The minimum TARC values of -8.272 dB, -8.223 dB, and -8.035 dB over the relevant bandwidth are calculated for these cases, which are slightly higher than -10 dB. The reported TARC values (~ -8 dB) are above the commonly accepted threshold of -10 dB for good MIMO performance. This shows that a large portion of incident power is reflected back, which reduces the overall efficiency and degrades the multiplexing capability of the antenna. Although the obtained TARC values still demonstrate acceptable multiport operation, the performance may not be optimal for high-efficiency MIMO applications. Also, the TARC values lie within the same range obtained with matched, open, and short loads, respectively.

The MEG$_k$ results for k=1, 2, 3, and 4 for Port= 1, 2, 3, and 4 are presented in Fig. 5(d), along with the MEG ratios between the dual ports. The MEG ratios are within ±3 dB across 4-6 GHz. Similar to the TARC values, negligible differences have been observed in the MEG values when connecting the matched, open, and short loads.

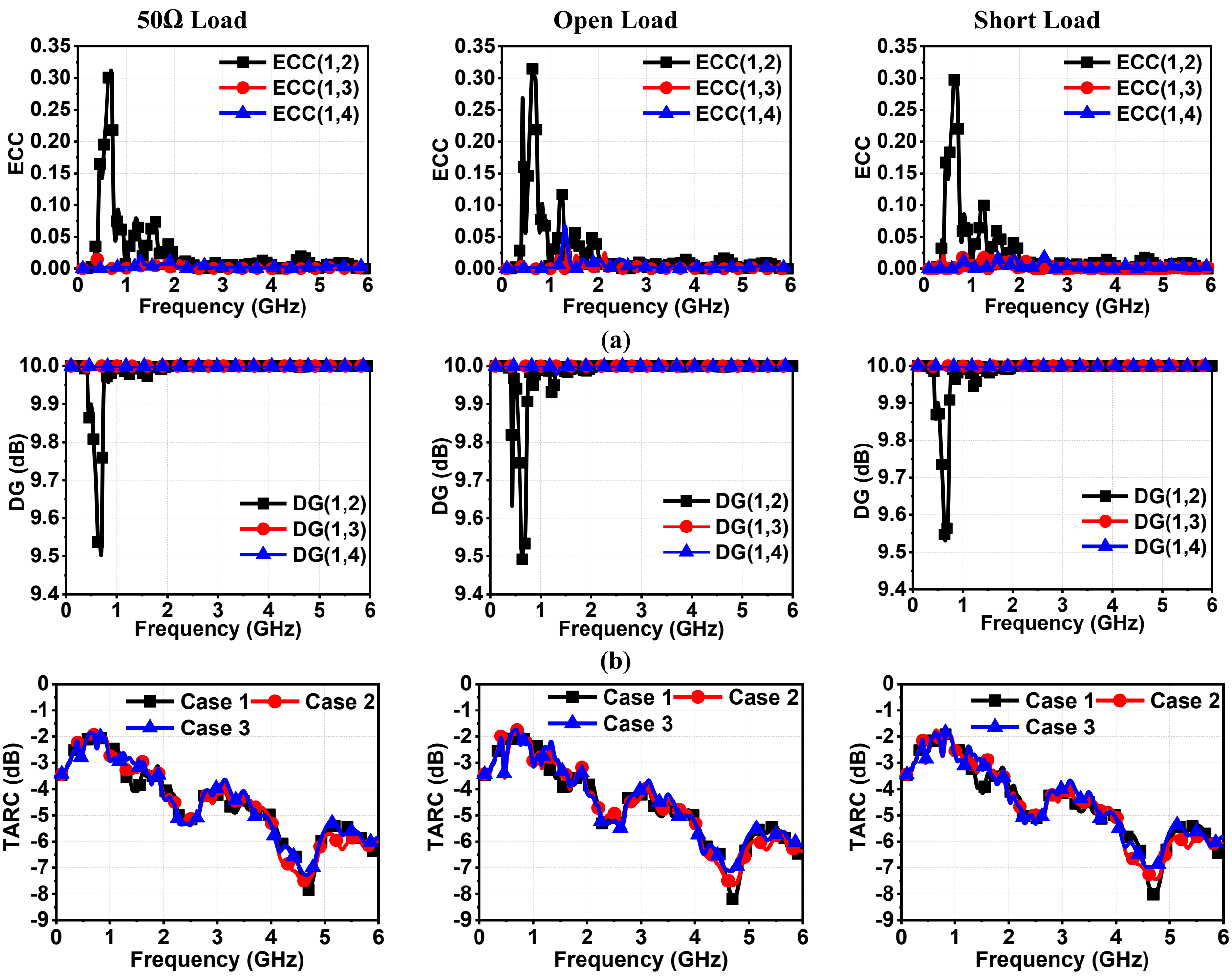

(c)

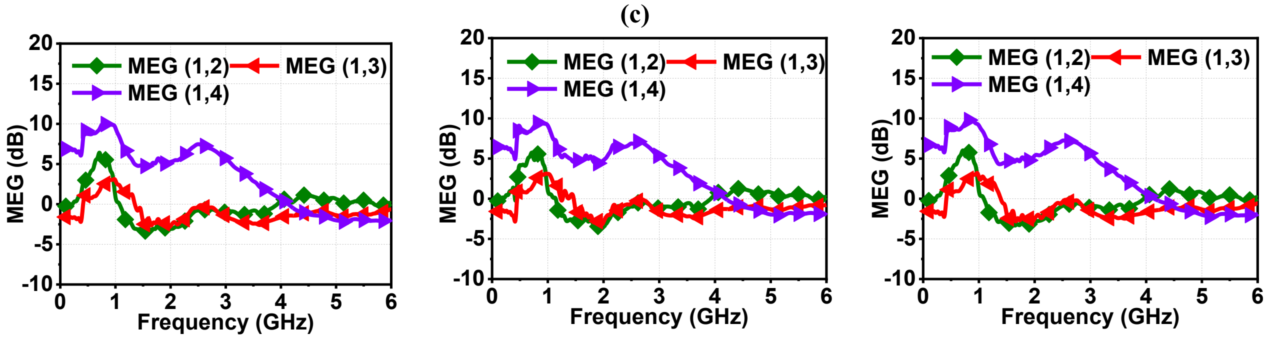

(d)

Figure 5: Diversity response of multi-band antenna under different loads (a) ECC, (b) DG, (c) TARC, and (d) MEG.

3. Conclusions:

In this work, the effect of different loads on the diversity parameters of the multiband MIMO antenna is investigated. The open and short loads increase reflection at the respective antenna ports and affect the reflection and transmission in a multiport system. Thus, both degrade the current distribution, transmission independence, and channel orthogonality in MIMO systems; hence, proper termination is critical for maintaining low ECC and high diversity gain. In the case of the multiband antenna, where each antenna element operates in a different frequency band, the variation in loads at the unused ports has no significant effect on diversity parameters.

Acknowledgements:

Authors are thankful to the Faculty Research Programme (FRP) of the Institute of Eminence (IoE), University of Delhi (Letter Ref. /No./IoE/2025-26/12/FRP dated 30.10.2025) for financial support.

Conflict of Interest:

Authors declare no conflicts of interest.

References:

[1] Puneet Sehgal, Kamlesh Patel, "Triband Dual Port h-SRR MIMO Antenna for WLAN/WiMAX/Wi-Fi 6 Applications," *Progress In Electromagnetics Research M,* vol. 123, pp. 35-43, 2024.

[2] Shailesh, G. Srivastava, S. Kumar, S. Ibrahim Alshathri, W. El-Shafai and O. Prakash Kumar, "Compact UWB MIMO Antenna With a Modified Back Reflector and Supported by Characteristic Mode Analysis for Wireless Communication Applications," *IEEE Access,* vol. 12, pp. 187302-187312, 2024.

[3] Shailesh, G. Srivastava, M. Al-Hamami, S. Kumar, S. M. P and O. P. Kumar, "Triple-Band Notched and Highly Decoupled MIMO Antenna Using Characteristic Mode Analysis," *IEEE Access,* vol. 13, pp. 165956-165969, 2025.

[4] Shailesh, S,M. Patel, and K. Patel, "Performance of 4 × 4 ring decoupling structure-based UWB MIMO antennas for transceiver applications in

simultaneous transmit and receive configuration," *Optical and Quantum Electronics,* vol. 58, p. 271, 2026.

[5] A. Srivastava et al., "Performance of two-element meander line MIMO antenna for Wi-Fi Internet of Things applications," *Journal of Electromagnetic Waves and Applications,* vol. 39, no. 14, pp. 1718-1734, 2025.

[6] M. K. Khan, S. Liu, and M. I. Khan, "A Wideband Eight-Port MIMO Antenna with Reduced Mutual Coupling for Future 5G mm-Wave Applications," *Sensors,* vol. 25, no. 2, p. 484, 2025.

[7] A. Kumar, A. Q. Ansari, B.K. Kanaujia, J. Kishor, and S. Kumar, "An Ultra-Compact Two-Port UWB-MIMO Antenna with Dual Band-Notched Characteristics," *AEU-International Journal of Electronics and Communications,* vol. 114, p. 152997, 2020.

[8] A. K. Chaudhary and M. Manohar, "A Modified SWB Hexagonal Fractal Spatial Diversity Antenna With High Isolation Using Meander Line Approach," *IEEE Access,* vol. 10, pp. 10238-10250, 2022.

[9] C. Yu et al., "A Super-Wideband and High Isolation MIMO Antenna System Using a Windmill-Shaped Decoupling Structure," *IEEE Access,* vol. 8, pp. 115767-115777, 2020.

[10] Sasmita Pahadsingh, Sudhakar Sahu, "Four port MIMO integrated antenna system with DRA for cognitive radio Platforms," *AEU - International Journal of Electronics and Communications,* vol. 92, pp. 98-110, 2018.